
UniQA: Unified Vision-Language Pre-training for Image Quality and Aesthetic Assessment

Hantao Zhou^{1,*}, Longxiang Tang^{1,*}, Rui Yang¹, Guanyi Qin¹, Yan Zhang³
Runze Hu^{2,†}, Xiu Li^{1,†}

¹Tsinghua University ²Beijing Institute of Technology ³Xiamen University
hantaozh@outlook.com, {lloong.x, rayyang0116}@gmail.com
qgy21@mails.tsinghua.edu.cn, {bzhy986, hrz1pk2015}@gmail.com,
li.xiu@sz.tinghua.edu.cn

Abstract

Image Quality Assessment (IQA) and Image Aesthetic Assessment (IAA) aim to simulate human subjective perception of image visual quality and aesthetic appeal. Existing methods typically address these tasks independently due to distinct learning objectives. However, they neglect the underlying interconnectedness of both tasks, which hinders the learning of task-agnostic shared representations for human subjective perception. To confront this challenge, we propose **Unified vision-language pre-training of Quality and Aesthetics (UniQA)**, to learn general perceptions of two tasks, thereby benefiting them simultaneously. Addressing the absence of text in the IQA datasets and the presence of textual noise in the IAA datasets, (1) we utilize multimodal large language models (MLLMs) to generate high-quality text descriptions; (2) the generated text for IAA serves as metadata to purify noisy IAA data. To effectively adapt the pre-trained UniQA to downstream tasks, we further propose a lightweight adapter that utilizes versatile cues to fully exploit the extensive knowledge of the pre-trained model. Extensive experiments demonstrate that our approach attains a new state-of-the-art performance on both IQA and IAA tasks, while concurrently showcasing exceptional zero-shot and few-label image assessment capabilities. The source code will be available at <https://github.com/zht8506/UniQA>.

1 Introduction

The advent of the mobile internet has empowered users worldwide to swiftly and easily share images. Presently, images dominate various social media platforms. The visual quality and aesthetics serve as crucial factors that aid these platforms in delivering high-quality images to users, thereby enhancing user experience. Furthermore, these aspects can effectively guide individuals in image photography and editing. Consequently, the Image Quality Assessment (IQA)² and Image Aesthetic Assessment (IAA), which can automatically measure the perceived quality and beauty of an image, are highly important and desired.

IQA and IAA concentrate on distinct aspects of image assessment, with IQA primarily focusing on the distortion level of the image, while IAA is oriented towards evaluating the aesthetic appeal of the image. Due to this divergence, most current works address these tasks independently, enhancing model performance by designing deeper and more sophisticated networks for either the IQA or IAA task. However, these approaches often overlook the underlying commonality between tasks: **simulating human subjective perceptions of images**.

Specifically, in human subjective evaluation of images, quality and aesthetics exhibit a mutual influence, such that high-quality images tend to possess a higher aesthetic appeal compared to

*Equal contribution. †Corresponding authors.

²The IQA in this work refers to the no-reference image quality assessment.

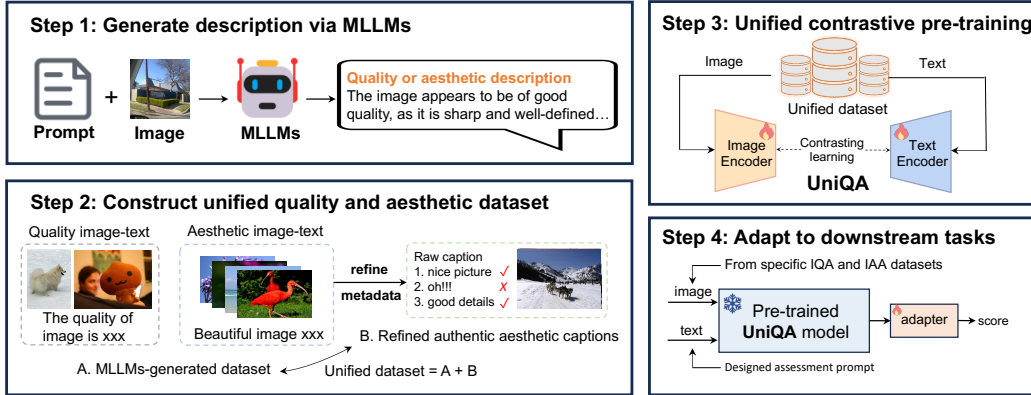


Figure 1: The overview of our method. We leverage MLLMs to generate quality- and aesthetics-related descriptions (Step 1) and utilize the generated data to refine authentic noisy data (Step 2). We conduct unified pre-training to obtain UniQA (Step 3), which can be flexibly applied to both IQA and IAA tasks with a lightweight adapter (Step 4).

their low-quality counterparts. Thus, the learning process for both tasks not only acquires features unique to themselves but also involves the learning of task-agnostic common representations. This commonality sparks an idea:

Can we develop a foundational model with robust visual assessment perceptions consistent with human to benefit both IQA and IAA tasks?

To achieve this, we propose the **Unified** pre-training of **Quality** and **Aesthetics** (UniQA) to learn general perceptions that align with human subjective image assessment. Different from some works [1, 2] that also attempt to jointly evaluate image quality and aesthetics, our UniQA learns powerful image assessment representations through pre-training, thereby more effectively boosting performance in both IQA and IAA tasks.

A straightforward pre-training solution involves consolidating all IQA and IAA datasets and then training the model to regress towards the mean opinion scores (MOS) annotated by humans. However, existing datasets show variations in perceptual scales due to differences in subjective testing methodologies [3]. As a result, this training strategy makes the model develop a score bias toward larger scale datasets. Moreover, it may not effectively capture the unique characteristics of IQA and IAA, as the MOS labels cannot be explicitly interpreted. To this end, we propose to use **text descriptions** as a bridge to integrate the two tasks, leveraging the rich and fine-grained semantics inherent in text to provide more auxiliary information.

However, to the best of our knowledge, existing IQA datasets [4–10] lack text descriptions. Conversely, although current IAA datasets [11] include text data provided by humans, they often contain considerable noise. Therefore, a top priority is determining how to acquire high-quality image-text data for both IQA and IAA tasks. Recently, multimodal large language models (MLLMs) [12–17] have demonstrated outstanding capabilities in image understanding, which can generate reasonable responses based on images and user instructions. Inspired by this, we propose utilizing MLLMs with tailored prompts to generate quality- and aesthetics-related descriptions for the IQA and IAA datasets, respectively (Step 1 of Fig. 1). As observed in Fig. 2, this approach provides a comprehensive and precise depiction of image quality and aesthetics. Furthermore, we utilize these generated high-quality aesthetics-related descriptions as metadata to refine the raw aesthetic caption dataset (Step 2 of Fig. 1). Finally, we unify the generated and refined image-text datasets to conduct vision-language contrast pre-training (Step 3 of Fig. 1). This results in the pre-trained UniQA with a powerful multimodal image assessment perception.

After pre-training on image-text pairs, we propose a lightweight adapter, namely the Multi-Cue Integration Adapter, to fine-tune the specific dataset of two tasks (Step 4 of Fig. 1). This adapter uses versatile cues related to image assessment to prompt the pre-trained UniQA, adeptly extracting useful knowledge and comprehensively assessing the image. With much fewer tunable parameters compared to previous IQA and IAA models, our model outperforms them on both tasks and also demonstrates exceptional performance in zero-shot and few-label image assessment settings.

Our contributions can be summarized as follows:

- With the assistance of MLLMs, we construct a high-quality image-text dataset about image quality and aesthetics. Through pre-training on this dataset, we develop UniQA, which effectively learns a general perception of image assessment, promoting the effective and efficient learning of both IQA and IAA tasks.
- We propose a novel Multi-Cue Integration Adapter, which integrates various assessment-related cues to fully exploit the extensive knowledge of the pre-trained model with minimal additional parameters.
- Extensive experiments show that our method achieves SOTA performance across multiple IQA and IAA datasets. Benefiting from the rich representations learned through pre-training, UniQA demonstrates exceptional zero-shot and few-label image assessment capabilities.

2 Related Work

Image Quality Assessment. The rapid development of deep learning has sparked significant interest in their application for IQA. Early works mainly utilize CNN to solve the IQA problem with various effective techniques, including deeper feature learning networks [18], multi-level feature aggregation [19], adaptive quality prediction [20], and patch-to-picture learning [9]. Recently, transformer methods [21–27] show promising results in the IQA field, which can compensate for the non-local representation ability of CNN. Despite these impressive breakthroughs, these methods often transfer models pre-trained on classification datasets, such as ImageNet [28], to IQA tasks, which may be suboptimal [29]. Our method can learn more effective representations through joint pre-training on quality-aesthetics image-text data, providing benefits for IQA tasks.

Image Aesthetic Assessment. With the advent of deep learning, IAA methods have evolved from hand-crafted feature extraction [30–34] to end-to-end feature learning, marking significant advancements in the IAA domain. Various techniques have been developed to boost IAA task, including local and global feature integration [35, 36], graph network [37, 38] and theme-aware learning [39, 40]. Recently, there has been an emergence of multimodal IAA methods [41–43] that incorporate text as auxiliary supervision. However, these methods necessitate the use of text during inference, limiting their flexible application since text is often not easily available. Our method overcomes this limitation by leveraging the rich semantics in text through vision-language pre-training. The pre-trained model can be flexibly applied to the IAA field using only images.

Vision-Language Models. Vision-Language Models (VLMs) [44–48] introduce the contrastive learning strategy to acquire image-text correspondences from large-scale image-text pairs. VLMs have exhibited promising results across multiple tasks [49, 50], including IQA [51, 52] and IAA [53, 54]. Recently, the Multimodal Large Language Models (MLLMs) have garnered increasing research interest, exhibiting remarkable prowess in comprehending image content and reasoning through complex instructions [12, 13, 55, 15–17, 56]. Most existing MLLMs achieve this by integrating image features with LLM tokens, subsequently fine-tuning the LLM via multimodal instruction tuning. During inference, MLLMs can reason with given images and user instructions, generating text responses by leveraging world knowledge learned during pre-training.

3 UniQA: MLLMs-assisted Unified Pre-training

In this section, we first present some preliminaries of related models (Sec. 3.1). We then describe the process of constructing a unified image-text dataset about quality and aesthetics, with the assistance of MLLMs (Sec. 3.2 and 3.3). We use this dataset to pre-train the vision-language model (Sec. 3.4), resulting in UniQA with powerful multimodal image assessment perception.

3.1 Preliminaries

Vision-language pre-training aims to achieve comprehensive cross-modality understanding by training on web-scale image-text datasets. Benefiting from this large-scale pre-training, CLIP [44], a prominent VLM, has demonstrated great promise to assist a broad scope of vision tasks. Specifically,

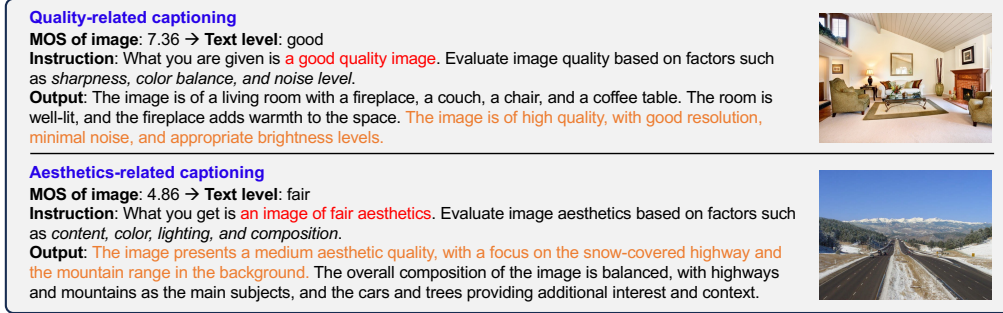


Figure 2: Generated quality- and aesthetics-related captions via MLLMs. The **red text** refers to MOS-based text guidance. The **orange text** highlights the quality- and aesthetics-related text.

CLIP comprises an image encoder f and a text encoder g , both jointly trained to establish a shared latent space for image and text through contrastive learning.

Given a batch of N paired images and texts $\{x_I^i, x_T^i\}_{i=1}^N$, CLIP extracts image features $I = \{f(x_I^i)\}_{i=1}^N$ and text features $T = \{g(x_T^i)\}_{i=1}^N$ with corresponding encoders. During pre-training, CLIP seeks to maximize the cosine similarity of paired image and text features, while minimizing the similarity of unmatched pairs. The contrastive learning objective can be formulated as:

$$\begin{aligned} \mathcal{L}_{\text{image}} &= -\mathbb{E}_{I_i \sim I} \left[\log \frac{\exp(I_i^\top T_i / \tau)}{\sum_{j=1}^N \exp(I_i^\top T_j / \tau)} \right] \\ \mathcal{L}_{\text{text}} &= -\mathbb{E}_{T_i \sim T} \left[\log \frac{\exp(T_i^\top I_i / \tau)}{\sum_{j=1}^N \exp(T_i^\top I_j / \tau)} \right] \end{aligned} \quad (1)$$

where the I_i and T_i are the i -th features in the batch, and τ is the temperature parameter. The final contrastive learning loss can be obtained by taking the average: $\mathcal{L} = (\mathcal{L}_{\text{image}} + \mathcal{L}_{\text{text}})/2$. With this training strategy, CLIP can generate aligned features in latent space for paired image-text samples.

3.2 Quality- and Aesthetics-related Captioning

In order to achieve vision-language pre-training in the field of image assessment, we need to generate text for IQA and IAA datasets since IQA datasets lack text and IAA datasets contain noisy text. Recently, MLLMs have shown advanced performance, so we can use them to generate high-quality textual data for images. Previous studies [57, 58] have highlighted that it is challenging for MLLMs to directly and accurately perceive the quality and aesthetics of input images, often resulting in positively skewed expressions and strong hallucinations. Thus, to obtain correct and fine-grained descriptions about quality and aesthetics, we provide an open-sourced MLLM (M_T) with a task-specific prompt P_t and a *MOS-based text guidance* G , attaining a large number of captions Y_t :

$$Y_t \sim M_T(x_I, P_t | G). \quad (2)$$

To obtain G , we divide images into 5 levels based on MOS, *i.e.*, {bad, poor, fair, good, perfect} [8, 4, 52]. If an image’s MOS ranks in the top 20% of the score range, its level is assigned to perfect. This approach standardizes IQA and IAA datasets with different scales, alleviating the MOS biases of different datasets [3]. Additionally, P_t is customized for IQA (P_{IQA}) and IAA (P_{IAA}) tasks, respectively. As shown in Fig. 2, P_{IQA} involves *sharpness, color balance, and noise level* [59], while P_{IAA} includes *content, color, lighting, and composition* [60]. With these designs, M_T is guided towards image assessment and we can obtain generated caption datasets Y_{IQA} and Y_{IAA} for IQA and IAA task, respectively.

3.3 Data Purification

In addition to the generated aesthetic captions Y_{IAA} , there are also IAA datasets with captions commented by humans [11], which directly reflect human aesthetic feelings. Incorporating comments from various people can offer a more comprehensive description of image aesthetics. However, while enhancing text diversity, it may introduce noise to the data, as individuals may provide comments

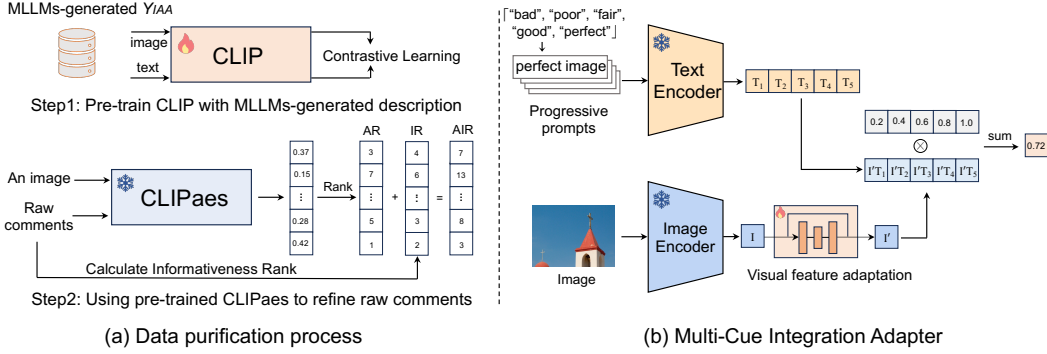


Figure 3: (a) Data purification process: we pre-train CLIP using generated aesthetic captions data Y_{IAA} and then use the pre-trained $CLIP_{aes}$ to purify data. (b) The proposed adapter: we employ progressive prompts, {bad, poor, fair, good, perfect} with “image”, to prompt the frozen UniQA and a lightweight trainable module to adjust visual features.

unrelated to image aesthetics. To address this issue, we propose a novel data purification strategy to refine raw captions in the original dataset. This process is illustrated in Fig. 3(a).

Specifically, we introduce Aesthetics-relevance and Informativeness Rank (AIR) to measure the quality of text corresponding to an image. The AIR consists of Aesthetics-relevance Rank (AR) and Informativeness Rank (IR). To obtain AR, we first pre-train a CLIP model with generated aesthetic data Y_{IAA} to get an aesthetics-aware CLIP model, denoted as $CLIP_{aes}$. Then, we employ it to measure the aesthetics relevance score (s_A) for an image-text pair. Given an image with n captions, AR can be defined as:

$$AR = \text{Rank}(s_A^1 \cdots s_A^n), \quad s_A^i = \text{CLIP}_{aes}(x_I, x_T^i), \quad (3)$$

where s_A^i represents the aesthetics relevance score between the i -th caption x_T^i and its corresponding image x_I . Note that AR consists of *long integers* that represent the rank of a caption after sorting by s_A . To obtain IR, we simply utilize the sentence length as informativeness score (s_I) to measure the informativeness of text. Accordingly, for an image with n textual captions, IR can be expressed as:

$$IR = \text{Rank}(s_I^1, \cdots, s_I^n), \quad s_I^i = \text{Length}(x_T^i), \quad (4)$$

where $\text{Length}(\cdot)$ is able to output the length of an input sentence. As a result, AIR between an image and n captions is:

$$AIR = \text{Rank}((AR^1 + IR^1), \cdots, (AR^n + IR^n)). \quad (5)$$

We select captions with Top-K ranking AIR to construct a high-quality aesthetic caption dataset, denoted as Y_{IAA}^+ . This strategy ensures the preservation of text that is both related to aesthetic perception and rich in information, thereby enhancing the quality and richness of the raw dataset.

3.4 Unified Vision-Language Pre-training

So far, we have gotten a high-quality image-text dataset about quality and aesthetics, $Y = Y_{IQA} \cup Y_{IAA} \cup Y_{IAA}^+$. Based on it, we pre-train CLIP using Equation 1 to obtain our UniQA. In this way, the model learns general perceptions of image quality and aesthetics, which can provide potent assessment priors and thus can be effectively applied to both IQA and IAA tasks.

4 Adapting Vision-Language Model for IQA and IAA

The pre-trained UniQA contains extensive perception information, which can facilitate downstream assessment tasks in a zero-shot or supervised manner. In this section, we further propose a meticulously designed adapter (Sec. 4.1) and prompt engineering (Sec. 4.2) to enhance the model’s performance.

4.1 Multi-Cue Integration Adapter

During pre-training, the model aligns image and assessment-related captions, empowering it with strong comprehension of image quality and aesthetics. With this foundation model, we can slightly

adjust the visual features, efficiently adapting it to score-based image assessment tasks. To this end, we introduce a lightweight adapter, namely the Multi-Cue Integration Adapter, to adapt visual features and inject rich cues for fine-tuning downstream tasks. The adapter consists of two key processes: visual feature adaptation and multi-cue integration prediction.

Visual Feature Adaptation. We add a learnable residual module following the pre-trained image encoder to adjust the visual features so as to adapt to specific assessment datasets. We optimize this module while keeping the image and text backbones frozen, enabling parameter-efficient tuning. The structure of the adapter is illustrated in Fig. 3(b). Let I denote the image features extracted from the frozen image encoder, the visual feature adaptation process can be expressed as:

$$I' = \text{Normalize}(\text{Adapter}(I) + I) \quad (6)$$

where the $\text{Adapter}(\cdot)$ consists of two fully connected layers with a ReLU activation in between, and I' represents the adapted visual features.

Multi-cue Integration Prediction. A straightforward approach to incorporating the CLIP model into perception assessment is to utilize the “good image” as an anchor and take the cosine similarity between the text anchor and a given image as the assessment score. However, this method shows two shortcomings: 1) using the absolute value of similarity as the perception score may not be optimal because it only reflects the semantic similarity between images and texts [57, 51]; 2) a single prompt may not fully leverage the extensive knowledge of the pre-trained model. Thus, we propose to utilize versatile cues to comprehensively explore the power of the pre-trained UniQA and convert absolute similarity scores into relative values for weighting.

Specifically, we utilize the prompt template “{level} image” and five text levels in Sec. 3.2, *i.e.*, {bad, poor, fair, good, perfect}, to construct prompts. Next, we calculate the cosine similarity between the normalized text features $\{T_i\}_{i=1}^5$ of five prompts and adapted visual features I' , and then use the $\text{Softmax}(\cdot)$ to obtain the related value of five image-text correspondence. These related values will weight the predefined score levels to get the final assessment score. This process can be formulated as follows:

$$q = \sum_{i=1}^5 \frac{c_i \exp(I'^{\top} T_i / \tau)}{\sum_{j=1}^5 \exp(I'^{\top} T_j / \tau)}, \quad (7)$$

where $\{c_i\}_{i=1}^5$ are scores of text levels with progressive values that are set to $\{0.2, 0.4, 0.6, 0.8, 1.0\}$; τ is the temperature parameter and q is the assessment score of the given image.

4.2 Prompt Ensemble Strategy

We introduce the prompt ensemble strategy, which incorporates more prompt groups to derive the final assessment score, thereby achieving a more comprehensive understanding of image quality and aesthetics. For instance, we can use *e.g.*, {extremely blurry, blurry, fair, sharp, extremely sharp} as another five text levels. Now, the final assessment score q_f is the average of all prompt groups and it can be described as:

$$q_f = \frac{\sum_{i=1}^m q_i}{m}, \quad (8)$$

where m denotes the number of prompt groups. This strategy can more fully utilize the multi-modal understanding capabilities of the pre-trained UniQA and demonstrates non-negligible performance improvements in zero-shot (Tab. 4) and few-label supervised learning (Tab. 5). The details of ensemble prompts are attached in supplementary material.

5 Experiments

5.1 Datasets

We employ the IQA dataset FLIVE [9] and the IAA dataset AVA [61] for quality- and aesthetics-related captioning, respectively, and AVA-Captions [11] to provide authentic aesthetic comments. We evaluate the performance on typical IQA and IAA datasets, including seven IQA datasets and two IAA datasets.

Table 1: Results on IQA datasets. **Black** and **blue** numbers in bold represent the best and second best, respectively. Higher SRCC and PLCC imply better performance.

Method	TID2013		CSIQ		KADID		CLIVE		KonIQ		SPAQ	
	SRCC	PLCC	SRCC	PLCC	SRCC	PLCC	SRCC	PLCC	SRCC	PLCC	SRCC	PLCC
WaDIQaM [18]	0.835	0.855	0.852	0.844	0.739	0.752	0.682	0.671	0.804	0.807	0.840	0.845
DBCNN [67]	0.816	0.865	0.946	0.959	0.851	0.856	0.851	0.869	0.875	0.884	0.911	0.915
MetaIQA [68]	0.856	0.868	0.899	0.908	0.762	0.775	0.802	0.835	0.850	0.887	-	-
PaQ-2-PiQ [9]	0.862	0.856	0.899	0.902	0.840	0.849	0.844	0.842	0.872	0.885	-	-
HyperIQA [20]	0.840	0.858	0.923	0.942	0.852	0.845	0.859	0.882	0.906	0.917	0.911	0.915
TReS [69]	0.863	0.883	0.922	0.942	0.859	0.858	0.846	0.877	0.915	0.928	-	-
MUSIQ [21]	0.773	0.815	0.871	0.893	0.875	0.872	0.702	0.746	0.916	0.928	0.918	0.921
DEIQT [22]	0.892	0.908	0.946	0.963	0.889	0.887	0.875	0.894	0.921	0.934	0.919	0.923
LIQE [52]	-	-	0.936	0.939	0.930	0.931	0.904	0.911	0.919	0.908	-	-
Ours	0.916	0.931	0.963	0.973	0.940	0.943	0.890	0.905	0.933	0.941	0.924	0.928

Table 2: Results on AVA dataset.

Method	SRCC	PLCC
NIMA [70]	0.612	0.636
MaxViT [71]	0.708	0.745
APM [72]	0.709	-
MUSIQ [21]	0.726	0.738
MLSP [73]	0.756	0.757
TANet [40]	0.758	0.765
EAT [74]	0.759	0.77
VILA [75]	0.774	0.774
Ours	0.776	0.776

Table 3: Results on AADB dataset.

Method	SRCC	PLCC
NIMA [70]	0.708	0.711
MLSP [73]	0.725	0.726
MUSIQ [21]	0.706	0.712
PA-IAA [76]	0.720	0.728
HIAA [77]	0.739	-
TANet [40]	0.738	0.737
Celona <i>et al.</i> [78]	0.757	0.762
TAVAR [39]	0.761	0.763
Ours	0.786	0.787

Table 4: SRCC on the zero-shot setting. * denotes using ensemble prompts. The results of other methods are pre-trained on FLIVE.

Method	CLIVE	KonIQ	AGIQA-3K
DBCNN	0.724	0.716	0.645
PaQ-2-PiQ	0.738	0.755	0.502
HyperIQA	0.735	0.758	0.629
DEIQT	0.781	0.733	-
CLIP*	0.746	0.592	0.646
Ours	0.638	0.667	0.744
Ours*	0.790	0.806	0.752

IQA Dataset. For the IQA task, four synthetic datasets, including LIVE [4], CSIQ [5], TID2013 [62], KADID [6], and three authentic datasets of CLIVE [8], KonIQ [7], SPAQ [10], are used for performance evaluation. FLIVE [9] is an authentic IQA dataset that contains 39,810 images. We employ an AIGC-generated IQA dataset, AGIQA-3K [63], to evaluate the generalization capability of our UniQA. Details of the datasets can be found in the supplementary material.

IAA Dataset. For the IAA task, we conduct experiments on AVA [61] and AADB [64] datasets. AVA comprises 250k images, with the test set of 19,928 images. AADB dataset consists of 10,000 images in total, with 8,500 images for training, 500 images for validation, and 1,000 images for testing.

AVA-Captions Dataset. AVA-Captions [11] offer multiple human-annotated comments for each AVA image. To avoid potential data leakage, we strictly follow the official data split of AVA, results in a pre-training image-text dataset comprising 234,090 images paired with 3.0 million captions.

5.2 Implementation Details

We use CLIP-B/16 [44] as our VLM for pre-training and LLaVA-1.5-7B [12, 65] as our MLLM for captioning. We pre-train the model using Adam optimizer [66] with a learning rate of $5e-6$ and weight decay of 0.2. The model is trained for 5 epochs with a batch size of 960. We set $K = 4$ to refine the AVA-Captions dataset. We use MSE loss to optimize the adapter on downstream tasks and different training settings according to the task and size of datasets. More training details are provided in the appendix. For each IQA dataset, 80% of the images are used for training and the remaining 20% for testing. We repeat this process 10 times to mitigate the performance bias and the medians of SRCC and PLCC are reported. For the IAA datasets, we follow the standard data splits.

5.3 Main Results

Results on IQA task. Tab. 1 reports the performance of the SOTA IQA methods on six typical IQA datasets. The results of LIVE [4] are presented in the supplementary material due to page limitations. Our method demonstrates a substantial superiority over existing SOTA models across a diverse range of datasets, fully confirming the effectiveness and excellence of our method in precisely characterizing image quality.

Results on IAA task. We report the experimental results on the AVA [61] and AADB [64] datasets in Tab. 2 and Tab. 3, respectively. Given that the pre-trained model acquired a unified and robust

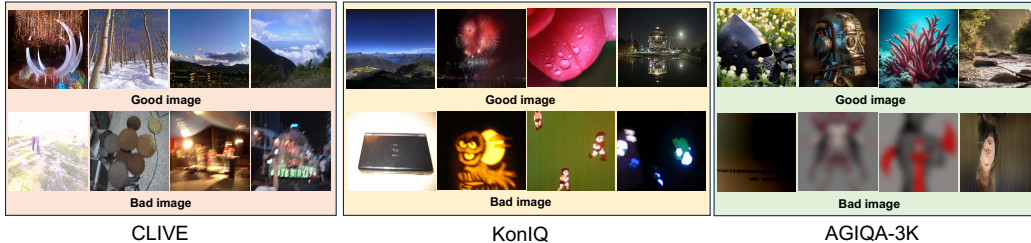


Figure 4: The image retrieval results on three dataset with varied prompts. Zoom in for a better view.

Table 5: SRCC results using few labels for training. * denotes using ensemble prompts.

Method	CLIVE			KonIQ			LIVE		
	50	100	200	50	100	200	50	100	200
HyperIQA [20]	0.648	0.725	0.790	0.615	0.710	0.776	0.892	0.912	0.929
TReS [69]	0.670	0.751	0.799	0.713	0.719	0.791	0.901	0.927	0.957
ResNet50 [79]	0.576	0.611	0.636	0.635	0.670	0.707	0.871	0.906	0.922
CLIP [44]	0.664	0.721	0.733	0.736	0.770	0.782	0.896	0.923	0.941
CONTRIQUE [80]	0.695	0.729	0.761	0.733	0.794	0.821	0.891	0.922	0.943
Re-IQA [81]	0.591	0.621	0.701	0.685	0.723	0.754	0.884	0.894	0.929
DEIQT [22]	0.667	0.718	0.812	0.638	0.682	0.754	0.920	0.942	0.955
GRepQ [82]	0.760	0.791	0.822	0.812	0.832	0.855	0.926	0.937	0.953
Ours	0.813	0.836	0.850	0.772	0.842	0.870	0.962	0.956	0.974
Ours*	0.828	0.849	0.853	0.844	0.860	0.876	0.963	0.958	0.976

image assessment perception, it can also achieve SOTA results after fine-tuning on these two datasets. These results validate that our method can be effectively applied to both IQA and IAA domains.

5.4 Generalization Capability Validation

Tab. 4 evaluate the generalization capability of our model. Unlike previous methods that train on one dataset and test on others, we directly utilize the pre-trained UniQA and textual prompts for image quality assessment. This presents a more challenging setting as the model isn’t optimized on MOS labels. As observed, our method achieves the best performance on these three datasets. Notably, our method demonstrates excellent performance on AIGC-generated images AGIQA-3K [63], which are markedly different from images of natural scenes. These results demonstrate the strong generalization capability of our UniQA. Additionally, the UniQA outperforms the original CLIP significantly, proving the effectiveness of our quality- and aesthetics-related pre-training.

We use different text queries to calculate the image-text similarity and rank them to achieve zero-shot image retrieval. Fig. 4 demonstrates the visualization of the top retrieval results. We notice that the retrieved results of “good image” exhibit sharp and aesthetically pleasing images, whereas “bad image” prompts retrieve blurry, poor lighting and meaningless images. These examples provide qualitative evidence of the quality and aesthetic knowledge captured by the pre-trained model.

5.5 Data-Efficient Learning

The pre-trained model acquires extensive image assessment knowledge, providing robust priors for downstream tasks. Consequently, our model can deliver impressive performance with limited data. To validate this, we randomly select subsets of 50, 100, and 200 samples from the training set for training and evaluate them on the same test data as full-data supervised learning. We report the median performance across 10 times in Tab. 5. Our method notably outperforms the second-best model GRepQ by a substantial margin, even though GRepQ is specifically designed for data-efficient learning. These results thoroughly demonstrate the potent capability of our method to learn image quality even when only a few labels are available. Additionally, several insightful observations can be drawn from Tab. 5. Firstly, the prompt ensemble strategy markedly enhances model performance in the data-efficient setting. This is attributed to its ability to more fully leverage the extensive knowledge of the pre-trained model. Secondly, the impact of prompt ensemble is slight on synthetic datasets. This is likely due to the limited image variety within synthetic datasets, making a single prompt sufficient for such scenarios.

5.6 Ablation Studies

Impact of different pre-training data. Tab. 6 shows the effect of different pre-training data. We observe that unified pre-training achieves the optimal performance on both tasks. In addition, we derive some meaningful observations. First, using either the generated Y_{IQA} or Y_{IAA} improves the performance of both IQA and IAA tasks, proving the mutual benefit of these two tasks and the effectiveness of MLLMs captioning. Second, unifying Y_{IQA} and Y_{IAA} datasets does not lead to significant improvements. We believe this is because the MLLMs-generated text tends to have similar sentence structures [83] and perception representation, limiting the diversity provided for multimodal learning. Third, pre-training with refined authentic Y_{IAA}^+ shows significant improvement on two tasks, reflecting that human-annotated comments can provide a more comprehensive and effective representation for the model.

Effectiveness of data purification strategy. The second part of Tab. 6 illustrates the ablation study of the data purification strategy. It can be observed that employing either AR or IR strategy to purify data can improve the model’s performance. These results validate the benefit of obtaining aesthetically relevant and semantically rich textual descriptions for the model. Finally, when combining these two strategies, it achieves the best performance.

Effectiveness of the Multi-Cue Integration Adapter. The third part of Tab. 6 shows the ablation study of the proposed adapter. “Single Prompt” denotes using the similarity between the text “good image” and images as the assessment score directly, while “Antonym Prompt” represents using the relative weights of texts “good image” and “bad image” to weight the predefined score. It is evident that the “Single Prompt” is considerably inferior to the “Antonym Prompt”, showing the limitations of using semantic similarity as score directly. Our method integrates more cues into the “Antonym Prompt” to comprehensively assess images, thereby achieving optimal performance.

Effectiveness of the Multi-Cue Integration Adapter. The bottom part of Tab. 6 presents the ablation study of various MLLMs. We generate Y_{IQA} via different MLLMs for pre-training. It is evident that using different MLLMs exhibits similar performance, while ensembling different MLLMs can boost performance. This indicates that MLLMs are capable of generating accurate captions with our text-guided prompt, and enhancing caption diversity can further improve performance. Considering resource limitations, we use LLaVa-7B and will integrate more MLLMs in the future.

6 Conclusion and Discussion

This paper introduces UniQA, which leverages unified vision-language pre-training to address quality and aesthetic assessment problems concurrently. We construct a high-quality image-text dataset about quality and aesthetics with the assistance of MLLMs. Through large-scale pre-training on this dataset, UniQA learns shared and effective representations of IQA and IAA tasks, benefiting both tasks. Additionally, we propose a Multi-Cue Integration Adapter to effectively adapt the pre-trained UniQA to downstream assessment tasks. Our method achieves state-of-the-art performance on both IQA and IAA tasks, and demonstrates powerful zero-shot and few-label image assessment capabilities.

Limitations and future work. MLLMs often generate captions with similar sentence structures and semantic expressions, restricting their ability to provide diverse and enriched representations for multimodal learning. Future work will explore other techniques to address this issue, including integrating various MLLMs for captioning and employing in-context learning methods.

Table 6: Ablation on IQA (CLIVE and KonIQ) and IAA (AVA) datasets with SRCC metrics.

Ablation type			CLIVE	KonIQ	AVA
Ablation on different pre-training data					
Y_{IQA}	Y_{IAA}	Y_{IAA}^+			
×	×	×	0.865	0.907	0.748
✓	×	×	0.871	0.914	0.755
×	✓	×	0.871	0.917	0.755
✓	✓	×	0.874	0.918	0.756
×	×	✓	0.875	0.928	0.773
×	✓	✓	0.877	0.930	0.774
✓	✓	✓	0.890	0.933	0.776
Ablation on data purification strategy					
w/o Strategy			0.876	0.929	0.772
IR Strategy			0.879	0.931	0.774
AR Strategy			0.885	0.930	0.774
AIR Strategy			0.890	0.933	0.776
Ablation on the proposed adapter					
Single Prompt			0.705	0.920	0.765
Antonym Prompt			0.875	0.928	0.771
Ours adapter			0.890	0.933	0.776
Ablation on different MLLMs					
LLaVA-v1.5-7B			0.871	0.914	0.755
LLaVA-v1.5-13B			0.872	0.914	0.757
Sphinx			0.874	0.916	0.758
QWen-VL			0.870	0.913	0.757
LLaVa-7B+QWen			0.875	0.916	0.758
Sphinx+QWen			0.877	0.918	0.759

References

- [1] Kaiwei Zhang, Dandan Zhu, Xiongkuo Min, Zhongpai Gao, and Guangtao Zhai. Synergetic assessment of quality and aesthetic: Approach and comprehensive benchmark dataset. *IEEE TCSVT*, 2023.
- [2] Franz Götz-Hahn, Lai-Kuan Wong, and Vlad Hosu. The inter-relationship between photographic aesthetics and technical quality. In *Modeling Visual Aesthetics, Emotion, and Artistic Style*, pages 231–255. Springer, 2023.
- [3] Weixia Zhang, Kede Ma, Guangtao Zhai, and Xiaokang Yang. Uncertainty-aware blind image quality assessment in the laboratory and wild. *IEEE TIP*, 30:3474–3486, 2021.
- [4] Hamid R Sheikh, Muhammad F Sabir, and Alan C Bovik. A statistical evaluation of recent full reference image quality assessment algorithms. *IEEE TIP*, 15(11):3440–3451, 2006.
- [5] Eric C Larson and Damon M Chandler. Most apparent distortion: full-reference image quality assessment and the role of strategy. *Journal of electronic imaging*, 19(1):011006–011006, 2010.
- [6] Hanhe Lin, Vlad Hosu, and Dietmar Saupe. Kadid-10k: A large-scale artificially distorted iqa database. In *2019 Eleventh International Conference on Quality of Multimedia Experience (QoMEX)*, pages 1–3. IEEE, 2019.
- [7] Vlad Hosu, Hanhe Lin, Tamas Sziranyi, and Dietmar Saupe. Koniq-10k: An ecologically valid database for deep learning of blind image quality assessment. *IEEE TIP*, 29:4041–4056, 2020.
- [8] Deepti Ghadiyaram and Alan C Bovik. Massive online crowdsourced study of subjective and objective picture quality. *IEEE TIP*, 25(1):372–387, 2015.
- [9] Zhenqiang Ying, Haoran Niu, Praful Gupta, Dhruv Mahajan, Deepti Ghadiyaram, and Alan Bovik. From patches to pictures (paq-2-piq): Mapping the perceptual space of picture quality. In *CVPR*, pages 3575–3585, 2020.
- [10] Yuming Fang, Hanwei Zhu, Yan Zeng, Kede Ma, and Zhou Wang. Perceptual quality assessment of smartphone photography. In *CVPR*, pages 3677–3686, 2020.
- [11] Koustav Ghosal, Aakanksha Rana, and Aljosa Smolic. Aesthetic image captioning from weakly-labelled photographs. In *ICCV Workshops*, pages 0–0, 2019.
- [12] Haotian Liu, Chunyuan Li, Qingyang Wu, and Yong Jae Lee. Visual instruction tuning. *arXiv preprint arXiv:2304.08485*, 2023.
- [13] Deyao Zhu, Jun Chen, Xiaoqian Shen, Xiang Li, and Mohamed Elhoseiny. Minigpt-4: Enhancing vision-language understanding with advanced large language models. *arXiv preprint arXiv:2304.10592*, 2023.
- [14] Ziyi Lin, Chris Liu, Renrui Zhang, Peng Gao, Longtian Qiu, Han Xiao, Han Qiu, Chen Lin, Wenqi Shao, Keqin Chen, et al. Sphinx: The joint mixing of weights, tasks, and visual embeddings for multi-modal large language models. *arXiv preprint arXiv:2311.07575*, 2023.
- [15] Bo Li, Yuanhan Zhang, Liangyu Chen, Jinghao Wang, Jingkang Yang, and Ziwei Liu. Otter: A multi-modal model with in-context instruction tuning. *arXiv preprint arXiv:2305.03726*, 2023.
- [16] Qinghao Ye, Haiyang Xu, Guohai Xu, Jiabo Ye, Ming Yan, Yiyang Zhou, Junyang Wang, Anwen Hu, Pengcheng Shi, Yaya Shi, et al. mplug-owl: Modularization empowers large language models with multimodality. *arXiv preprint arXiv:2304.14178*, 2023.
- [17] Jinze Bai, Shuai Bai, Shusheng Yang, Shijie Wang, Sinan Tan, Peng Wang, Junyang Lin, Chang Zhou, and Jingren Zhou. Qwen-vl: A versatile vision-language model for understanding, localization, text reading, and beyond. 2023.
- [18] Sebastian Bosse, Dominique Maniry, Klaus-Robert Müller, Thomas Wiegand, and Wojciech Samek. Deep neural networks for no-reference and full-reference image quality assessment. *IEEE TIP*, 27(1):206–219, 2017.

- [19] Dingquan Li, Tingting Jiang, Weisi Lin, and Ming Jiang. Which has better visual quality: The clear blue sky or a blurry animal? *IEEE TMM*, 21(5):1221–1234, 2018.
- [20] Shaolin Su, Qingsen Yan, Yu Zhu, Cheng Zhang, Xin Ge, Jinqiu Sun, and Yanning Zhang. Blindly assess image quality in the wild guided by a self-adaptive hyper network. In *CVPR*, pages 3667–3676, 2020.
- [21] Junjie Ke, Qifei Wang, Yilin Wang, Peyman Milanfar, and Feng Yang. Musiq: Multi-scale image quality transformer. In *ICCV*, pages 5148–5157, 2021.
- [22] Guanyi Qin, Runze Hu, Yutao Liu, Xiawu Zheng, Haotian Liu, Xiu Li, and Yan Zhang. Data-efficient image quality assessment with attention-panel decoder. *arXiv preprint arXiv:2304.04952*, 2023.
- [23] Longxiang Tang, Kai Li, Chunming He, Yulun Zhang, and Xiu Li. Consistency regularization for generalizable source-free domain adaptation. In *ICCVW*, pages 4323–4333, 2023.
- [24] Hantao Zhou, Rui Yang, Runze Hu, Chang Shu, Xiaochu Tang, and Xiu Li. Etdnet: efficient transformer-based detection network for surface defect detection. *IEEE Transactions on Instrumentation and Measurement*, 2023.
- [25] Hantao Zhou, Rui Yang, Yachao Zhang, Haoran Duan, Yawen Huang, Runze Hu, Xiu Li, and Yefeng Zheng. Unihead: unifying multi-perception for detection heads. *arXiv preprint arXiv:2309.13242*, 2023.
- [26] Junyong You and Jari Korhonen. Transformer for image quality assessment. In *ICIP*, pages 1389–1393. IEEE, 2021.
- [27] Mengmeng Zhu, Guanqun Hou, Xinjia Chen, Jiaying Xie, Haixian Lu, and Jun Che. Saliency-guided transformer network combined with local embedding for no-reference image quality assessment. In *ICCV*, pages 1953–1962, 2021.
- [28] Jia Deng, Wei Dong, Richard Socher, Li-Jia Li, Kai Li, and Li Fei-Fei. Imagenet: A large-scale hierarchical image database. In *CVPR*, pages 248–255. IEEE, 2009.
- [29] Xudong Li, Timin Gao, Xiawu Zheng, Runze Hu, Jingyuan Zheng, Yunhang Shen, Ke Li, Yutao Liu, Pingyang Dai, Yan Zhang, et al. Adaptive feature selection for no-reference image quality assessment using contrastive mitigating semantic noise sensitivity. *arXiv preprint arXiv:2312.06158*, 2023.
- [30] Ritendra Datta, Dhiraj Joshi, Jia Li, and James Z Wang. Studying aesthetics in photographic images using a computational approach. In *ECCV*, pages 288–301. Springer, 2006.
- [31] Yan Ke, Xiaoou Tang, and Feng Jing. The design of high-level features for photo quality assessment. In *CVPR*, volume 1, pages 419–426. IEEE, 2006.
- [32] Masashi Nishiyama, Takahiro Okabe, Imari Sato, and Yoichi Sato. Aesthetic quality classification of photographs based on color harmony. In *CVPR*, pages 33–40. IEEE, 2011.
- [33] Xiaoshuai Sun, Hongxun Yao, Rongrong Ji, and Shaohui Liu. Photo assessment based on computational visual attention model. In *ACM MM*, pages 541–544, 2009.
- [34] Wei Luo, Xiaogang Wang, and Xiaoou Tang. Content-based photo quality assessment. In *ICCV*, pages 2206–2213. IEEE, 2011.
- [35] Xin Lu, Zhe Lin, Xiaohui Shen, Radomir Mech, and James Z Wang. Deep multi-patch aggregation network for image style, aesthetics, and quality estimation. In *ICCV*, pages 990–998, 2015.
- [36] Jingwen Hou, Sheng Yang, and Weisi Lin. Object-level attention for aesthetic rating distribution prediction. In *ACM MM*, pages 816–824, 2020.
- [37] Dongyu She, Yu-Kun Lai, Gaoxiong Yi, and Kun Xu. Hierarchical layout-aware graph convolutional network for unified aesthetics assessment. In *CVPR*, pages 8475–8484, 2021.

- [38] Jiachen Duan, Pengfei Chen, Leida Li, Jinjian Wu, and Guangming Shi. Semantic attribute guided image aesthetics assessment. In *2022 IEEE International Conference on Visual Communications and Image Processing (VCIP)*, pages 1–5. IEEE, 2022.
- [39] Leida Li, Yipo Huang, Jinjian Wu, Yuzhe Yang, Yaqian Li, Yandong Guo, and Guangming Shi. Theme-aware visual attribute reasoning for image aesthetics assessment. *IEEE TCSVT*, 2023.
- [40] Shuai He, Yongchang Zhang, Rui Xie, Dongxiang Jiang, and Anlong Ming. Rethinking image aesthetics assessment: Models, datasets and benchmarks. In *IJCAI*, pages 942–948, 2022.
- [41] Xiaodan Zhang, Xinbo Gao, Wen Lu, Lihuo He, and Jie Li. Beyond vision: A multimodal recurrent attention convolutional neural network for unified image aesthetic prediction tasks. *IEEE TMM*, 23:611–623, 2020.
- [42] Ye Zhou, Xin Lu, Junping Zhang, and James Z Wang. Joint image and text representation for aesthetics analysis. In *ACM MM*, pages 262–266, 2016.
- [43] Xiaodan Zhang, Xinbo Gao, Lihuo He, and Wen Lu. Mscan: Multimodal self-and-collaborative attention network for image aesthetic prediction tasks. *Neurocomputing*, 430:14–23, 2021.
- [44] Alec Radford, Jong Wook Kim, Chris Hallacy, Aditya Ramesh, Gabriel Goh, Sandhini Agarwal, Girish Sastry, Amanda Askell, Pamela Mishkin, Jack Clark, et al. Learning transferable visual models from natural language supervision. In *ICML*, pages 8748–8763. PMLR, 2021.
- [45] Chao Jia, Yinfei Yang, Ye Xia, Yi-Ting Chen, Zarana Parekh, Hieu Pham, Quoc Le, Yun-Hsuan Sung, Zhen Li, and Tom Duerig. Scaling up visual and vision-language representation learning with noisy text supervision. In *ICML*, pages 4904–4916. PMLR, 2021.
- [46] Lewei Yao, Runhui Huang, Lu Hou, Guansong Lu, Minzhe Niu, Hang Xu, Xiaodan Liang, Zhenguo Li, Xin Jiang, and Chunjing Xu. Filip: Fine-grained interactive language-image pre-training. *arXiv preprint arXiv:2111.07783*, 2021.
- [47] Jiahui Yu, Zirui Wang, Vijay Vasudevan, Legg Yeung, Mojtaba Seyedhosseini, and Yonghui Wu. Coca: Contrastive captioners are image-text foundation models. *arXiv preprint arXiv:2205.01917*, 2022.
- [48] Quan Sun, Yuxin Fang, Ledell Wu, Xinlong Wang, and Yue Cao. Eva-clip: Improved training techniques for clip at scale. *arXiv preprint arXiv:2303.15389*, 2023.
- [49] Jiawei Yao, Qi Qian, and Juhua Hu. Multi-modal proxy learning towards personalized visual multiple clustering. *arXiv preprint arXiv:2404.15655*, 2024.
- [50] Yicheng Xiao, Zhuoyan Luo, Yong Liu, Yue Ma, Hengwei Bian, Yatai Ji, Yujiu Yang, and Xiu Li. Bridging the gap: A unified video comprehension framework for moment retrieval and highlight detection. *arXiv preprint arXiv:2311.16464*, 2023.
- [51] Jianyi Wang, Kelvin CK Chan, and Chen Change Loy. Exploring clip for assessing the look and feel of images. In *AAAI*, volume 37, pages 2555–2563, 2023.
- [52] Weixia Zhang, Guangtao Zhai, Ying Wei, Xiaokang Yang, and Kede Ma. Blind image quality assessment via vision-language correspondence: A multitask learning perspective. In *CVPR*, pages 14071–14081, 2023.
- [53] Simon Hentschel, Konstantin Kobs, and Andreas Hotho. Clip knows image aesthetics. *Frontiers in Artificial Intelligence*, 5:976235, 2022.
- [54] Xiangfei Sheng, Leida Li, Pengfei Chen, Jinjian Wu, Weisheng Dong, Yuzhe Yang, Liwu Xu, Yaqian Li, and Guangming Shi. Aesclip: Multi-attribute contrastive learning for image aesthetics assessment. In *ACM MM*, pages 1117–1126, 2023.
- [55] Danny Driess, Fei Xia, Mehdi SM Sajjadi, Corey Lynch, Aakanksha Chowdhery, Brian Ichter, Ayaan Wahid, Jonathan Tompson, Quan Vuong, Tianhe Yu, et al. Palm-e: An embodied multimodal language model. *arXiv preprint arXiv:2303.03378*, 2023.

- [56] Rui Yang, Lin Song, Yanwei Li, Sijie Zhao, Yixiao Ge, Xiu Li, and Ying Shan. Gpt4tools: Teaching large language model to use tools via self-instruction. *NeurIPS*, 36, 2024.
- [57] Haoning Wu, Zicheng Zhang, Erli Zhang, Chaofeng Chen, Liang Liao, Annan Wang, Chunyi Li, Wenxiu Sun, Qiong Yan, Guangtao Zhai, et al. Q-bench: A benchmark for general-purpose foundation models on low-level vision. *arXiv preprint arXiv:2309.14181*, 2023.
- [58] Yipo Huang, Quan Yuan, Xiangfei Sheng, Zhichao Yang, Haoning Wu, Pengfei Chen, Yuzhe Yang, Leida Li, and Weisi Lin. Aesbench: An expert benchmark for multimodal large language models on image aesthetics perception. *arXiv preprint arXiv:2401.08276*, 2024.
- [59] Damon M Chandler. Seven challenges in image quality assessment: past, present, and future research. *International Scholarly Research Notices*, 2013, 2013.
- [60] Yubin Deng, Chen Change Loy, and Xiaoou Tang. Image aesthetic assessment: An experimental survey. *IEEE Signal Processing Magazine*, 34(4):80–106, 2017.
- [61] Naila Murray, Luca Marchesotti, and Florent Perronnin. Ava: A large-scale database for aesthetic visual analysis. In *CVPR*, pages 2408–2415. IEEE, 2012.
- [62] Nikolay Ponomarenko, Oleg Ieremeiev, Vladimir Lukin, Karen Egiazarian, Lina Jin, Jaakko Astola, Benoit Vozel, Kacem Chehdi, Marco Carli, Federica Battisti, et al. Color image database tid2013: Peculiarities and preliminary results. In *European workshop on visual information processing (EUVIP)*, pages 106–111. IEEE, 2013.
- [63] Chunyi Li, Zicheng Zhang, Haoning Wu, Wei Sun, Xiongkuo Min, Xiaohong Liu, Guangtao Zhai, and Weisi Lin. Agiqa-3k: An open database for ai-generated image quality assessment. *arXiv preprint arXiv:2306.04717*, 2023.
- [64] Shu Kong, Xiaohui Shen, Zhe Lin, Radomir Mech, and Charless Fowlkes. Photo aesthetics ranking network with attributes and content adaptation. In *ECCV*, pages 662–679. Springer, 2016.
- [65] Haotian Liu, Chunyuan Li, Yuheng Li, and Yong Jae Lee. Improved baselines with visual instruction tuning. *arXiv preprint arXiv:2310.03744*, 2023.
- [66] Diederik P Kingma and Jimmy Ba. Adam: A method for stochastic optimization. *arXiv preprint arXiv:1412.6980*, 2014.
- [67] Weixia Zhang, Kede Ma, Jia Yan, Dexiang Deng, and Zhou Wang. Blind image quality assessment using a deep bilinear convolutional neural network. *IEEE TCSVT*, 30(1):36–47, 2018.
- [68] Hancheng Zhu, Leida Li, Jinjian Wu, Weisheng Dong, and Guangming Shi. Metaiqa: Deep meta-learning for no-reference image quality assessment. In *CVPR*, pages 14143–14152, 2020.
- [69] S Alireza Golestaneh, Saba Dadsetan, and Kris M Kitani. No-reference image quality assessment via transformers, relative ranking, and self-consistency. In *WACV*, pages 1220–1230, 2022.
- [70] Hossein Talebi and Peyman Milanfar. Nima: Neural image assessment. *IEEE TIP*, 27(8):3998–4011, 2018.
- [71] Zhengzhong Tu, Hossein Talebi, Han Zhang, Feng Yang, Peyman Milanfar, Alan Bovik, and Yinxiao Li. Maxvit: Multi-axis vision transformer. In *ECCV*, pages 459–479. Springer, 2022.
- [72] Naila Murray and Albert Gordo. A deep architecture for unified aesthetic prediction. *arXiv preprint arXiv:1708.04890*, 2017.
- [73] Vlad Hosu, Bastian Goldlucke, and Dietmar Saupe. Effective aesthetics prediction with multi-level spatially pooled features. In *CVPR*, pages 9375–9383, 2019.
- [74] Shuai He, Anlong Ming, Shuntian Zheng, Haobin Zhong, and Huadong Ma. Eat: An enhancer for aesthetics-oriented transformers. In *ACM MM*, pages 1023–1032, 2023.

- [75] Junjie Ke, Keren Ye, Jiahui Yu, Yonghui Wu, Peyman Milanfar, and Feng Yang. Vila: Learning image aesthetics from user comments with vision-language pretraining. In *CVPR*, pages 10041–10051, 2023.
- [76] Leida Li, Hancheng Zhu, Sicheng Zhao, Guiguang Ding, and Weisi Lin. Personality-assisted multi-task learning for generic and personalized image aesthetics assessment. *IEEE TIP*, 29:3898–3910, 2020.
- [77] Leida Li, Jiachen Duan, Yuzhe Yang, Liwu Xu, Yaqian Li, and Yandong Guo. Psychology inspired model for hierarchical image aesthetic attribute prediction. In *ICME*, pages 1–6. IEEE, 2022.
- [78] Luigi Celona, Marco Leonardi, Paolo Napoletano, and Alessandro Rozza. Composition and style attributes guided image aesthetic assessment. *IEEE TIP*, 31:5009–5024, 2022.
- [79] Kaiming He, Xiangyu Zhang, Shaoqing Ren, and Jian Sun. Deep residual learning for image recognition. In *CVPR*, pages 770–778, 2016.
- [80] Pavan C Madhusudana, Neil Birkbeck, Yilin Wang, Balu Adsumilli, and Alan C Bovik. Image quality assessment using contrastive learning. *IEEE TIP*, 31:4149–4161, 2022.
- [81] Avinab Saha, Sandeep Mishra, and Alan C Bovik. Re-iqa: Unsupervised learning for image quality assessment in the wild. In *CVPR*, pages 5846–5855, 2023.
- [82] Suhas Srinath, Shankhanil Mitra, Shika Rao, and Rajiv Soundararajan. Learning generalizable perceptual representations for data-efficient no-reference image quality assessment. In *WACV*, pages 22–31, 2024.
- [83] Yanqing Liu, Kai Wang, Wenqi Shao, Ping Luo, Yu Qiao, Mike Zheng Shou, Kaipeng Zhang, and Yang You. Mllms-augmented visual-language representation learning. *arXiv preprint arXiv:2311.18765*, 2023.
- [84] Anish Mittal, Anush Krishna Moorthy, and Alan Conrad Bovik. No-reference image quality assessment in the spatial domain. *IEEE TIP*, 21(12):4695–4708, 2012.
- [85] Lin Zhang, Lei Zhang, and Alan C Bovik. A feature-enriched completely blind image quality evaluator. *IEEE TIP*, 24(8):2579–2591, 2015.
- [86] Jongyoo Kim and Sanghoon Lee. Fully deep blind image quality predictor. *IEEE Journal of selected topics in signal processing*, 11(1):206–220, 2016.
- [87] Kede Ma, Wentao Liu, Kai Zhang, Zhengfang Duanmu, Zhou Wang, and Wangmeng Zuo. End-to-end blind image quality assessment using deep neural networks. *IEEE TIP*, 27(3):1202–1213, 2017.
- [88] Zhaoqing Pan, Hao Zhang, Jianjun Lei, Yuming Fang, Xiao Shao, Nam Ling, and Sam Kwong. Dacnn: Blind image quality assessment via a distortion-aware convolutional neural network. *IEEE TCSVT*, 32(11):7518–7531, 2022.
- [89] Ramprasaath R Selvaraju, Michael Cogswell, Abhishek Das, Ramakrishna Vedantam, Devi Parikh, and Dhruv Batra. Grad-cam: Visual explanations from deep networks via gradient-based localization. In *ICCV*, pages 618–626, 2017.

A Discussion about the AIR

We propose the Aesthetics-relevance and Informativeness Rank (AIR) to select the high-quality texts corresponding to an image. The AIR can be expressed as follows:

$$\text{AIR} = \text{Rank}((\text{AR}^1 + \text{IR}^1), \dots, (\text{AR}^n + \text{IR}^n)). \quad (9)$$

where AR and IR denote the Aesthetics-relevance Rank and Informativeness Rank, respectively; n is the number of comments corresponding to an image. For simplicity, we directly take the summation

of IR and AR to reflect the semantic relevance and richness of the text. In fact, we can introduce two factors (α and β) to purify the data more flexibly. Now, the modified AIR_m can be formulated as:

$$\text{AIR}_m = \text{Rank}((\alpha\text{AR}^1 + \beta\text{IR}^1), \dots, (\alpha\text{AR}^n + \beta\text{IR}^n)). \quad (10)$$

For instance, we can use large α for the highly noisy data. With this strategy, we can more flexibly purify data based on data quality.

Table 7: Details of different IQA datasets.

Dataset	Dataset Type	Dataset Size	Number of distortions
LIVE [4]	Synthetic	799	5
CSIQ [5]	Synthetic	866	5
TID2013 [62]	Synthetic	3,000	24
KADID [6]	Synthetic	10,125	25
CLIVE [8]	Authentic	1,162	-
KonIQ [7]	Authentic	10,073	-
SPAQ [10]	Authentic	11,000	-
FLIVE [9]	Authentic	39,810	-
AGIQA-3K [63]	Authentic	2,982	-

B Details of Datasets and Evaluation Criteria

We list the details of the datasets used in our work in Tab. 7, including the dataset type, dataset size and number of distortion types. Since the distortions of authentic datasets are diverse, their number cannot be counted.

We employ Spearman’s Rank-order Correlation Coefficient (SRCC) and Pearson’s Linear Correlation Coefficient (PLCC) as criteria to measure the performance of IQA and IAA models. They reflect the prediction monotonicity and prediction accuracy of the model, respectively. Both SRCC and PLCC range from 0 to 1. Higher values of SRCC and PLCC indicate better performance.

Table 8: Training settings for different datasets.

Dataset	Task	Epoch	Batch size	Learning rate
LIVE [4]	IQA	50	8	2e-4
CSIQ [5]	IQA	50	8	2e-4
TID2013 [62]	IQA	20	8	2e-4
KADID [6]	IQA	20	8	2e-4
CLIVE [8]	IQA	50	8	2e-4
KonIQ [7]	IQA	20	8	2e-4
SPAQ [10]	IQA	20	8	2e-4
AVA [61]	IAA	20	128	5e-4
AADB [64]	IAA	20	8	5e-4

C More Implementation Details

For the pre-training, we employ the same training strategy as CLIP [44] to pre-train our UniQA. The pre-training is resource-friendly and takes *less than an hour* at a time. When fine-tuning the adapter for downstream assessment tasks, we use different training settings according to the task and size of the dataset. Tab. 8 shows the detailed training setting for the different datasets. We follow the typical training strategy to fine-tune each dataset, including random cropping and random horizontal flipping. Since different datasets have different MOS scales, we scale their range to [0, 1] through normalization. During inference, we typically crop an input image into 10 image patches and take their average as the quality score of this image [20, 22]. We use the resolution of 224 × 224 for training and testing. All experiments are conducted on two A100 GPUs.

D Prompt Ensemble

Table 9: Text prompts used in zero-shot and few-label learning.

Task	Prompt
CLIVE, KonIQ, LIVE	{bad, poor, fair, good, perfect} with image
	{extremely blurry, blurry, fair, sharp, extremely sharp} with image
	{extremely noisy, noisy, fair, noise-free, extremely noise-free} with image
	{extremely low-quality, low-quality, fair, high-quality, extremely high-quality} with image
AGIQA-3K	{bad, poor, fair, good, perfect} with image {bad, poor, fair, good, perfect} with content

Table 11: PLCC performance comparison of our method with other NR-IQA methods trained using few labels. * denotes using ensemble prompts.

Method	LIVEC			KonIQ			LIVE		
	50	100	200	50	100	200	50	100	200
HyperIQA [20]	0.689	0.755	0.806	0.650	0.758	0.807	0.903	0.922	0.931
TReS [69]	0.702	0.776	0.813	0.740	0.748	0.824	0.916	0.948	0.960
ResNet50 [79]	0.580	0.629	0.660	0.661	0.693	0.716	0.872	0.908	0.920
CLIP [44]	0.676	0.739	0.758	0.749	0.790	0.802	0.891	0.924	0.942
CONTRIQUE [80]	0.693	0.736	0.777	0.743	0.801	0.832	0.892	0.922	0.944
Re-IQA [81]	0.620	0.650	0.701	0.689	0.693	0.757	0.876	0.892	0.931
DEIQT [22]	0.695	0.739	0.818	0.670	0.707	0.778	0.916	0.942	0.957
GRepQ [82]	0.772	0.798	0.835	0.793	0.816	0.840	0.929	0.936	0.957
Ours	0.819	0.854	0.866	0.815	0.861	0.890	0.952	0.959	0.970
Ours*	0.826	0.847	0.869	0.857	0.883	0.893	0.963	0.962	0.973

When applying our UniQA to zero-shot and few-label settings, prompt ensemble is a useful strategy to improve performance. Tab. 9 shows the prompt groups used in these two settings. Note that the prompts used in AGIQA-3K are different from other IQA datasets. This is because distortions in AIGC-generated images and authentic images tend to be different. For example, distortions in authentic images may come from camera shake. However, distortions in AIGC-generated images typically come from low-quality content, such as meaningless content and distorted poses. Therefore, we use “content” to prompt the pre-trained multimodal model for the AGIQA-3K dataset.

E More Experimental Results

E.1 Comparison Results on LIVE

Tab .10 shows the comparison results with other methods on LIVE dataset [4]. We can observe that our method also achieves state-of-the-art (SOTA) performance, verifying the effectiveness of our method.

E.2 PLCC Comparison in the Data-efficient Setting

The Pearson’s Linear Correlation Coefficient (PLCC) comparisons for our method against other IQA methods corresponding to the table in the main paper are provided in Tab .11. We note that our method outperforms all other methods in terms of PLCC metric.

Table 10: Results on LIVE dataset [4]. **Black** and **blue** numbers in bold represent the best and second best, respectively. Higher SRCC and PLCC imply better performance.

Method	LIVE	
	SRCC	PLCC
DIIVINE [18]	0.892	0.908
BRISQUE [84]	0.929	0.944
ILNIQE [85]	0.902	0.906
BIECON [86]	0.958	0.961
MEON [87]	0.951	0.955
WaDIQaM [18]	0.960	0.955
DBCNN [67]	0.968	0.971
MetaIQA [68]	0.960	0.959
PaQ-2-PiQ [9]	0.959	0.958
HyperIQA [20]	0.962	0.966
TReS [69]	0.969	0.968
MUSIQ [21]	0.940	0.911
DACNN [88]	0.978	0.980
DEIQT [22]	0.980	0.982
LIQE [52]	0.970	0.951
Ours	0.981	0.983

Table 12: Results on IQA datasets. **Black** and **blue** numbers in bold represent the best and second best, respectively. Higher SRCC and PLCC imply better performance.

Method	TID2013		CSIQ		KADID		CLIVE		KonIQ		SPAQ	
	SRCC	PLCC	SRCC	PLCC	SRCC	PLCC	SRCC	PLCC	SRCC	PLCC	SRCC	PLCC
DIIVINE [18]	0.643	0.567	0.804	0.776	0.413	0.435	0.588	0.591	0.546	0.558	0.599	0.600
BRISQUE [84]	0.626	0.571	0.812	0.748	0.528	0.567	0.629	0.629	0.681	0.685	0.809	0.817
ILNIQE [85]	0.521	0.648	0.822	0.865	0.534	0.558	0.508	0.508	0.523	0.537	0.712	0.713
BIECON [86]	0.717	0.762	0.815	0.823	0.623	0.648	0.613	0.613	0.651	0.654	-	-
MEON [87]	0.808	0.824	0.852	0.864	0.604	0.691	0.697	0.710	0.611	0.628	-	-
WaDIQaM [18]	0.835	0.855	0.852	0.844	0.739	0.752	0.682	0.671	0.804	0.807	0.840	0.845
DBCNN [67]	0.816	0.865	0.946	0.959	0.851	0.856	0.851	0.869	0.875	0.884	0.911	0.915
MetaIQA [68]	0.856	0.868	0.899	0.908	0.762	0.775	0.802	0.835	0.850	0.887	-	-
PaQ-2-PiQ [9]	0.862	0.856	0.899	0.902	0.840	0.849	0.844	0.842	0.872	0.885	-	-
HyperIQA [20]	0.840	0.858	0.923	0.942	0.852	0.845	0.859	0.882	0.906	0.917	0.911	0.915
TReS [69]	0.863	0.883	0.922	0.942	0.859	0.858	0.846	0.877	0.915	0.928	-	-
MUSIQ [21]	0.773	0.815	0.871	0.893	0.875	0.872	0.702	0.746	0.916	0.928	0.918	0.921
DACNN [88]	0.871	0.889	0.943	0.957	0.905	0.905	0.866	0.884	0.901	0.912	0.915	0.921
DEIQT [22]	0.892	0.908	0.946	0.963	0.889	0.887	0.875	0.894	0.921	0.934	0.919	0.923
LIQE [52]	-	-	0.936	0.939	0.930	0.931	0.904	0.911	0.919	0.908	-	-
Ours	0.916	0.931	0.963	0.973	0.940	0.943	0.890	0.905	0.933	0.941	0.924	0.928

E.3 More Comparison Results on IQA Datasets

To demonstrate the superiority of our method more comprehensively, we present more comparison results on the typical IQA datasets in Tab. 12.

E.4 More Results of Ablation Study

Tab. 13 shows the SRCC and PLCC results of the ablation study.

F Details and Discussion of MLLMs Captioning

Details of MLLMs Captioning. We use different numbers of captions for IQA and IAA tasks. Considering that the IQA data does not have textual descriptions, we generate three captions with different prompts via MLLMs for the IQA datasets. This method can improve the text diversity of IQA image-text data. For the IAA dataset, we generate one caption for each image because IAA datasets have a large amount of authentic text data. Details of the prompts for quality-related captioning are shown in Fig. 5.

Effectiveness of text guidance. We visualize the MLLMs-generated captions with/without text guidance to evaluate the effectiveness of text guidance. We take the captioning for IQA datasets as examples. As shown in Fig. 10, when the quality of image is high, the MLLMs can output correct caption (see example 1). *However, we can observe that the MLLMs will generate wrong captions when low-quality images are sent to MLLMs and the text guidance is not provided (see example 2-4 of Fig. 10).* As a result, the text guidance is useful and necessary for MLLMs captioning.

G More visualization

G.1 Grad-CAM visualization of Different Pre-training

Fig. 6 illustrates the Grad-CAM [89] visualization of different pre-training. We can notice that after quality-related pre-training, the model pays more attention to blurred subjects and noisy backgrounds. This effect becomes more pronounced with unified pre-training, underscoring the advantages of such a unified approach.

G.2 More Examples of Zero-shot Retrieval

We show more examples of zero-shot retrieval in Fig. 7, Fig. 8 and Fig. 9. We explore the model’s retrieval capabilities in terms of color and light. We can observe that the images of “Good color” show harmonious and vivid colors while the images of “Bad color” present messy colors. For the

Details of quality-related captioning

MOS of image: 6.71 → **Text level:** good

Instruction 1: What you are given is **a good quality image**. Evaluate image quality based on factors such as *sharpness, color balance, and noise levels*.

Output 1: The image is of three hot air balloons flying in the sky. The balloons are of different sizes and are positioned at various heights. The sky is clear and blue, providing a perfect backdrop for the balloons. **The resolution of the image is good, allowing for clear visibility of the balloons and their details. Overall, the image quality is excellent,** capturing the essence of the hot air balloons in flight.

Instruction 2: Giving you **a good quality image**. Describe the quality of an image based on visual descriptors such as *resolution, noise, brightness*.

Output 2: **The image is of good quality,** with a resolution that allows for clear visibility of the three hot air balloons flying in the sky. **The noise level is low, and the brightness of the scene is well-balanced, making it an enjoyable view.** Overall, the image is high quality and has clear content.

Instruction 3: This is **a good quality** (*sharpness, contrast, distortion*) image. Assuming you are a human observer, please describe your feelings when you see this image.

Output 2: As a human observer, **I would feel a sense of wonder and excitement upon seeing this image.** The two hot air balloons flying in the sky, each with a unique design, create a visually appealing and captivating scene. **The contrast between the vibrant colors of the balloons and the clear blue sky adds to the overall beauty of the image.**




Figure 5: Details of the prompts of quality-related captioning. We generate three captions for each IQA image using different prompts.

retrieval on light, the images of “Good light” are clear and well-lit and the images of “Bad light” demonstrate dimly lit environments and poor lighting. These visualization results further demonstrate the strong capability of our model in understanding concepts related to quality and aesthetics.

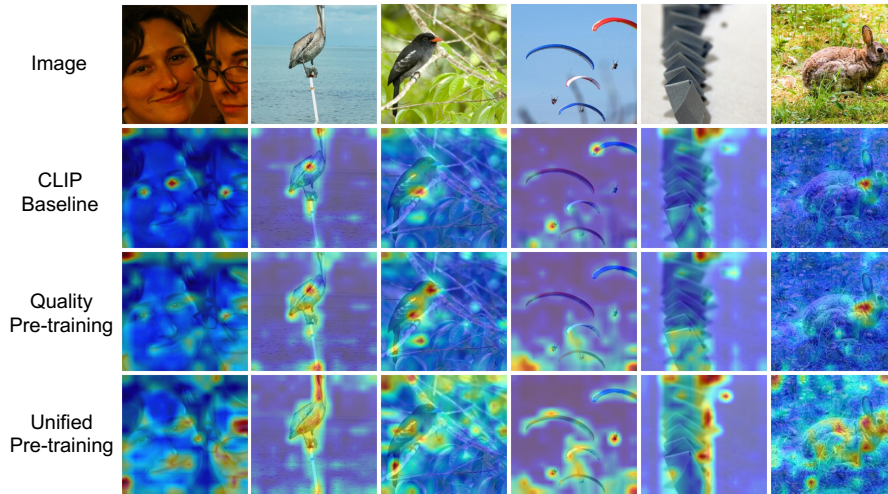


Figure 6: Grad-CAM [89] visualization of different pre-training for prompt “blurry image”. Through pre-training, the model focuses more on noisy objects and backgrounds.

G.3 Visualization of Data Purification Strategy

In Fig. 11, we visualize the comments sorted by the proposed strategies. As observed, the Aesthetics-relevance Rank (AR) can sort the aesthetics-related comments first. Further integrating the Informativeness Rank (IR), we can obtain aesthetically relevant comments with rich semantics.

G.4 More Examples of Text Generated by MLLMs

In Fig. 12, we show more examples of the captions generated by MLLMs. We can observe that with our prompt design, MLLMs can output correct fine-grained quality- and aesthetics-related descriptions.

Table 13: Ablation experiments on two IQA datasets (CLIVE and KonIQ) and one IAA dataset (AVA). Different ablations are distinguished by different backgrounds for better viewing.

Ablation type			CLIVE		KonIQ		AVA	
			SRCC	PLCC	SRCC	PLCC	SRCC	PLCC
Ablation on different pre-training data								
Y_{IQA}	Y_{IAA}	Y_{IAA}^+						
×	×	×	0.865	0.886	0.907	0.924	0.748	0.747
✓	×	×	0.871	0.898	0.914	0.932	0.755	0.755
×	✓	×	0.871	0.895	0.917	0.932	0.755	0.756
✓	✓	×	0.874	0.892	0.918	0.932	0.756	0.757
×	×	✓	0.875	0.895	0.928	0.937	0.773	0.774
×	✓	✓	0.877	0.895	0.930	0.939	0.774	0.774
✓	✓	✓	0.890	0.905	0.933	0.941	0.776	0.776
Ablation on data purification strategy								
w/o Strategy			0.876	0.899	0.929	0.940	0.772	0.771
IR Strategy			0.879	0.898	0.931	0.941	0.774	0.774
AR Strategy			0.885	0.901	0.930	0.942	0.774	0.773
AIR Strategy			0.890	0.905	0.933	0.941	0.776	0.776
Ablation on the proposed adapter								
Single Prompt			0.705	0.720	0.920	0.931	0.765	0.765
Antonym Prompt			0.875	0.897	0.928	0.938	0.771	0.772
Ours adapter			0.890	0.905	0.933	0.941	0.776	0.776
Ablation on different MLLMs								
LLaVA-v1.5-7B			0.871	0.898	0.914	0.932	0.755	0.755
LLaVA-v1.5-13B			0.872	0.897	0.914	0.929	0.757	0.759
Sphinx			0.874	0.902	0.916	0.931	0.758	0.758
QWen-VL			0.870	0.895	0.913	0.930	0.757	0.758
LLaVa-7B+QWen			0.875	0.899	0.916	0.930	0.758	0.757
Sphinx+QWen			0.877	0.908	0.918	0.934	0.759	0.760

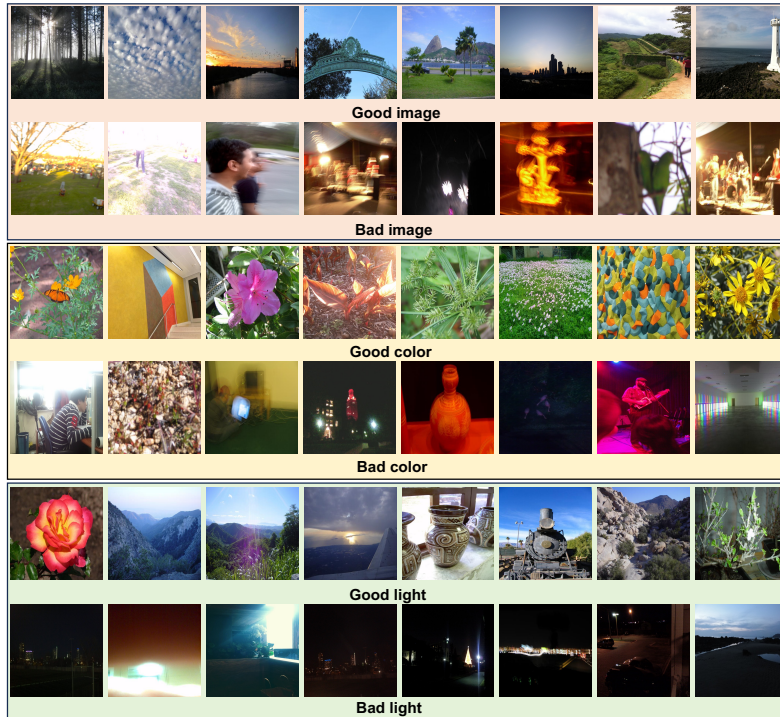


Figure 7: More image retrieval results with various text as queries on CLIVE [8].

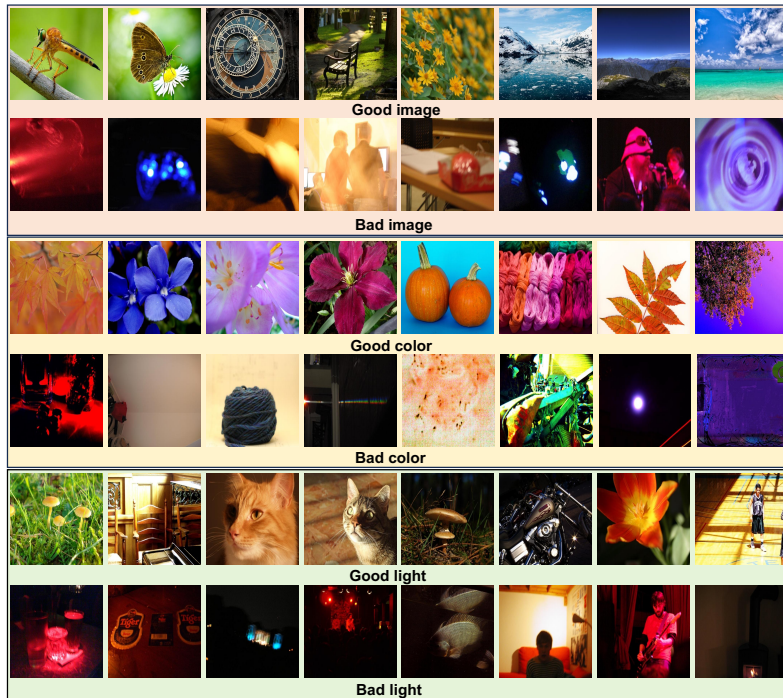


Figure 8: More image retrieval results with various text as queries on KonIQ [7].

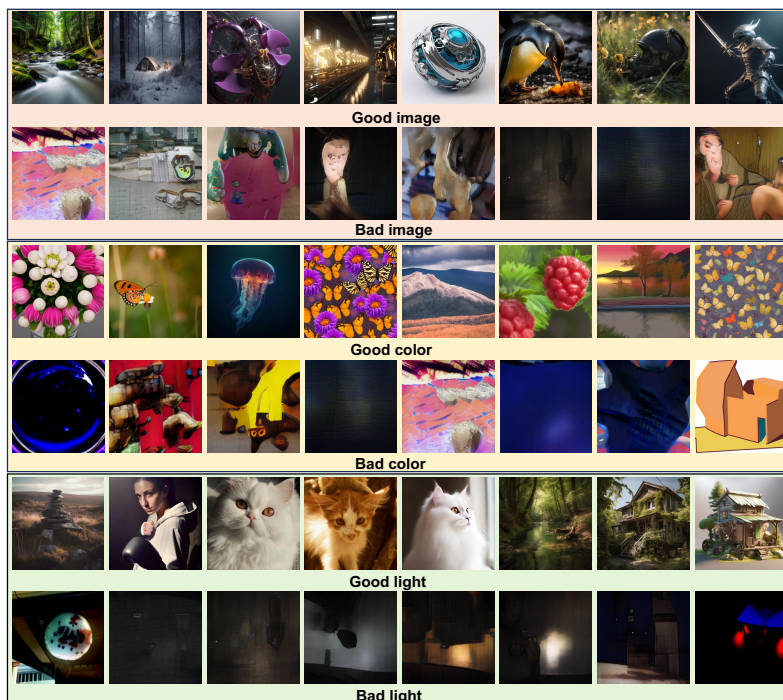


Figure 9: More image retrieval results with various text as queries on AGIQA-3K [63].

Example 1

Captioning with MOS-based text guidance

MOS of image: 8.82 → Text level: perfect

Instruction: What you are given is **a excellent quality image**. Evaluate image quality based on factors such as *sharpness, color balance, and noise level*.

Output: The image of the silver Canon camera is of high quality. The noise is minimal, and the brightness is well-balanced, making it an excellent representation of the camera. The composition of the image is well-executed, with the camera being the main focus, and the background is clean and uncluttered. Overall, the image showcases the camera's features and design effectively.



Captioning without MOS-based text guidance

Instruction: Evaluate image aesthetics based on factors such as *content, color, lighting, and composition*.

Output: The image quality of the silver digital camera is quite good. The camera appears to be sharp, with clear details visible in the image. The color balance is also well-maintained, with vibrant colors and accurate representation of the scene. Overall, the image quality of the camera is impressive, making it suitable for capturing high-quality photos and videos.

Example 2

Captioning with MOS-based text guidance

MOS of image: 3.91 → Text level: bad

Instruction: What you are given is **a bad quality image**. Evaluate image quality based on factors such as *sharpness, color balance, and noise level*.

Output: The camera appears to be in focus, but the overall quality of the image is poor. The brightness of the image is also low, which further contributes to the poor quality. The composition of the image is simple, with the camera being the main subject, and there are no other objects or elements in the frame.



Captioning without MOS-based text guidance

Instruction: Evaluate image aesthetics based on factors such as *content, color, lighting, and composition*.

Output: The camera appears to be in good condition, with no visible signs of damage or wear. The image quality seems to be quite good, as the camera appears to be sharp and well-focused. The color balance appears to be accurate, with no noticeable color distortions or over-saturation. Overall, the image quality seems to be quite good, with a well-focused, accurate color balance, and minimal noise.

Example 3

Captioning with MOS-based text guidance

MOS of image: 3.65 → Text level: bad

Instruction: What you are given is **a bad quality image**. Evaluate image quality based on factors such as *sharpness, color balance, and noise level*.

Output: The image quality is poor, with a low resolution that makes it difficult to discern details. The brightness of the image is also low, making it challenging to see the subject clearly. The composition of the image is somewhat interesting, featuring a Chinese-style roof structure with a sign on it, but the overall quality of the image is not satisfactory.



Captioning without MOS-based text guidance

Instruction: Evaluate image aesthetics based on factors such as *content, color, lighting, and composition*.

Output: The image quality appears to be quite good, with a sharp focus on the yellow and white sign. The colors in the image are well-balanced, and there is minimal noise, making it a visually appealing scene. The night sky in the background adds a sense of depth and contrast to the image, further enhancing its overall quality.

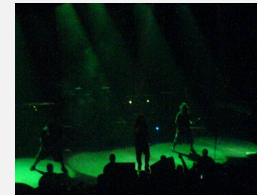
Example 4

Captioning with MOS-based text guidance

MOS of image: 1.01 → Text level: poor

Instruction: What you are given is **a poor quality image**. Evaluate image quality based on factors such as *sharpness, color balance, and noise level*.

Output: The image is of a concert with a group of people on stage. The resolution is low, which makes it difficult to discern the details of the performers and the audience. The brightness of the image is also low, making it hard to see the performers and the audience clearly. Overall, the image quality is poor due to low resolution, high noise, low brightness, and an unbalanced composition.



Captioning without MOS-based text guidance

Instruction: Evaluate image aesthetics based on factors such as *content, color, lighting, and composition*.

Output: The image quality appears to be quite good, with a high level of sharpness, color balance, and minimal noise. The image is a black and white photo of a band performing on stage, and the band members are clearly visible. The lighting in the scene is green, which adds a unique atmosphere to the image. Overall, the photo captures the essence of the live performance and the audience's engagement with the band.

Figure 10: Example of captioning with/without text guidance. The red text refers to MOS-based text guidance. The orange text highlights the correct quality-related caption. The green text indicates the incorrect quality-related caption without text guidance.



The Image

1. I really like this photo. I love the see-through globe. I like that the colours are so close to the ones used in the map below. It's a great composition.
2. Cool idea. I think the constellations should have been the focal point, and blur the earth globe a little bit. But great idea!
3. use a polarizer next time to get rid of the reflection... or wait.. I hear they don't work on plastic.
4. I can understand it as a zodiac shoot. Perhaps I know so much about it.
5. Cool. how did it look with the constellations being the focus?
6. Nice composition, DOF is about perfect, good color. Nice job!
7. Not sure this meets the challenge.
8. Thanks for all your comments!
9. Creative.

(1) IR strategy

1. I really like this photo. I love the see-through globe. I like that the colours are so close to the ones used in the map below. It's a great composition.
2. Cool idea. I think the constellations should have been the focal point, and blur the earth globe a little bit. But great idea!
3. Cool. how did it look with the constellations being the focus?
4. Nice composition, DOF is about perfect, good color. Nice job!
5. I can understand it as a zodiac shoot. Perhaps I know so much about it.
6. use a polarizer next time to get rid of the reflection... or wait.. I hear they don't work on plastic.
7. Thanks for all your comments!
8. Creative.
9. Not sure this meets the challenge.

(2) AR strategy

1. I really like this photo. I love the see-through globe. I like that the colours are so close to the ones used in the map below. It's a great composition.
2. Cool idea. I think the constellations should have been the focal point, and blur the earth globe a little bit. But great idea!
3. Cool. how did it look with the constellations being the focus?
4. I can understand it as a zodiac shoot. Perhaps I know so much about it.
5. use a polarizer next time to get rid of the reflection... or wait.. I hear they don't work on plastic.
6. Nice composition, DOF is about perfect, good color. Nice job!
7. Thanks for all your comments!
8. Not sure this meets the challenge.
9. Creative.

(3) AIR strategy



The Image

1. Ok, I have looked at this long and hard, even asked my wife and both of us could not figure any connection with the zodiac. So tell me what it is.. huh?
2. I like the sharp detail of the bare tree, but the background looks very unnatural and the frame seems too heavy for the picture.
3. I am still trying to relate to the challenge... Not quite sure... But the picture itself is beautiful! Nice tones.
4. I'm not sure how this relates to the challenge. I don't dislike this shot..in fact the colors are very appealing.
5. Nice picture, very artistic and postcard like, but I fail to see who does it meet the challenge.
6. Which zodiac sign is the tree? Nice picture but I don't see how it fits the challenge.
7. Love the dark sepia, but missing the Zodiac.
8. Love the composition, color, and exposure.
9. What symbol is this for?
10. zodiac?

(1) IR strategy

1. I am still trying to relate to the challenge... Not quite sure... But the picture itself is beautiful! Nice tones.
2. Love the dark sepia, but missing the Zodiac.
3. I like the sharp detail of the bare tree, but the background looks very unnatural and the frame seems too heavy for the picture.
4. Nice picture, very artistic and postcard like, but I fail to see who does it meet the challenge.
5. Which zodiac sign is the tree? Nice picture but I don't see how it fits the challenge.
6. Love the composition, color, and exposure.
7. I'm not sure how this relates to the challenge. I don't dislike this shot..in fact the colors are very appealing.
8. Ok, I have looked at this long and hard, even asked my wife and both of us could not figure any connection with the zodiac. So tell me what it is.. huh?
9. zodiac?
10. What symbol is this for?

(2) AR strategy

1. I am still trying to relate to the challenge... Not quite sure... But the picture itself is beautiful! Nice tones.
2. I like the sharp detail of the bare tree, but the background looks very unnatural and the frame seems too heavy for the picture.
3. Love the dark sepia, but missing the Zodiac.
4. Nice picture, very artistic and postcard like, but I fail to see who does it meet the challenge.
5. Ok, I have looked at this long and hard, even asked my wife and both of us could not figure any connection with the zodiac. So tell me what it is.. huh?
6. I'm not sure how this relates to the challenge. I don't dislike this shot..in fact the colors are very appealing.
7. Which zodiac sign is the tree? Nice picture but I don't see how it fits the challenge.
8. Love the composition, color, and exposure.
9. zodiac?
10. What symbol is this for?

(3) AIR strategy

Figure 11: The comments sorted using different strategies. With our proposed strategy, we can obtain aesthetically relevant and informative comments. The order of comments is determined by the corresponding strategy. Gray sentences indicate being filtered.

Quality-related captioning

MOS of image: 7.21 → **Text level:** good

Instruction: Giving you a **good quality image**. Describe the quality of an image based on visual descriptors such as *resolution*, *noise*, *brightness*.

Output: The image is of a green and yellow parrot sitting on a wooden perch. The bird appears to be looking at the camera, and its vibrant colors make it stand out in the scene. **The image is well-lit, with good contrast and resolution**, allowing for a clear view of the parrot's features.



MOS of image: 7.80 → **Text level:** good

Instruction: What you are given is a **good quality image**. Evaluate image quality based on factors such as *sharpness*, *color balance*, and *noise levels*.

Output: The image of the elephant in the grassy field is of good quality. **The resolution is high, allowing for clear details of the elephant's features**, such as its tusks and trunk. **The noise level is low**, resulting in a clean and unobstructed view of the elephant. **Overall, the image quality is excellent**, making it an appealing representation of the elephant in its natural habitat.



MOS of image: 2.73 → **Text level:** bad

Instruction: Giving you a **bad quality image**. Describe the quality of an image based on visual descriptors such as *resolution*, *noise*, *brightness*.

Output: **The image quality is poor, with a low resolution that makes it difficult to discern details**. The brightness is low, making it hard to see the pumpkin clearly. **The noise in the image is high, which adds to the overall poor quality**.

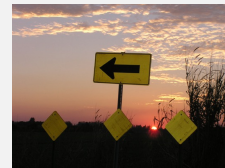


Aesthetics-related captioning

MOS of image: 5.09 → **Text level:** fair

Instruction: What you get is **an image of fair aesthetics**. Evaluate image aesthetics based on factors such as *content*, *color*, *lighting*, and *composition*.

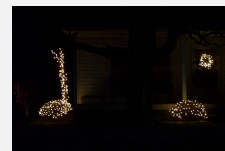
Output: **The image presents a visually appealing scene** with a combination of content, color, lighting, and composition. The sunset in the background creates a warm and serene atmosphere. **The combination of these elements results in an aesthetically pleasing image** that captures the viewer's attention and evokes a sense of tranquility.



MOS of image: 3.05 → **Text level:** bad

Instruction: What you get is **an image of bad aesthetics**. Evaluate image aesthetics based on factors such as *content*, *color*, *lighting*, and *composition*.

Output: In the image, there is a house with a lit-up Christmas tree in front of it. However, **the overall aesthetics of the image are not appealing** due to a few factors. Firstly, the tree is positioned in the foreground, occupying a significant portion of the frame, which can **make the image feel cramped and cluttered**. Secondly, the tree's lights are not evenly distributed, with some areas appearing brighter than others. This uneven lighting can create an unbalanced and unappealing visual effect.



MOS of image: 8.04 → **Text level:** perfect

Instruction: What you get is **an image of excellent aesthetics**. Evaluate image aesthetics based on factors such as *content*, *color*, *lighting*, and *composition*.

Output: **The image showcases an aesthetically pleasing scene of a lone tree standing in the middle of a grassy field at night**. The tree is illuminated by the moonlight, creating a serene and peaceful atmosphere. The night sky is filled with stars, adding to the beauty and tranquility of the scene. The composition of the image, with the tree as the focal point, draws the viewer's attention and invites them to appreciate the natural beauty of the landscape. **Overall, the image is visually appealing due to its content, color, lighting, and composition**.

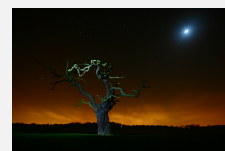


Figure 12: More examples of quality- and aesthetics-related captioning via MLLMs. The **red text** refers to MOS-based text guidance. The **orange text** highlights the quality- and aesthetics-related text.